J. Fluid Mech. (1976), *vol.* 73, *part* 4, *pp.* 621–639
Printed in Great Britain

Inviscid secondary motions in a tube of slowly varying ellipticity

By IAN J. SOBEY

Department of Applied Mathematics and Theoretical Physics,
University of Cambridge

(Received 24 June 1975)

Inviscid methods of treating secondary flows due to streamline curvature are well known in the literature. The development of secondary motions at high Reynolds number in a bifurcation characteristic of the lung airways or the cardiovascular system is considered. In particular, the secondary motions in the initial section of a bifurcation, which can be considered a tube of slowly varying ellipticity, are calculated. Providing viscous effects are confined to regions near the walls, the calculated velocity field agrees with experimental observation. Thus the structure of the secondary motions can be considered an effect of stretching of vortex lines by the tube boundary.

1. Introduction

The existence of secondary motions in engineering systems with internal fluid flow along curved streamlines is well known and has been extensively analysed by an inviscid theory. Methods of solving such inviscid problems were initiated by Squire & Winter (1951) and largely developed by Hawthorne (e.g. 1965) and Lighthill (1956). More recently Horlock & Lakshminarayana (1973) and Lakshminarayana & Horlock (1973) have reviewed and further expanded the theory of secondary flows. Such secondary flows arise for example in bent tubes and in flow through turbine blades.

These problems are tackled by assuming that the fluid is inviscid and initially carries vorticity normal to the direction of flow. The interaction of the flow with the downstream boundaries produces a deformation of the vortex lines as they are carried along streamlines of the flow. In this way vorticity in the direction of the flow is produced. It can be seen that such an explanation of the generation of secondary flows assumes that it is an inviscid effect arising from the deformation of vortex lines. At high Reynolds numbers viscosity would act to modify the inviscid flow, through the introduction of boundary layers at the walls, but in the absence of separation it is expected to have little effect elsewhere. All models do assume that separation does not occur.

The theory is based on the Cauchy–Helmholtz–Kelvin theorem that vortex lines move with the fluid, their strength changing with local stretching. An approximate method of solution proceeds as follows. We consider a basic, or 'primary', flow to transport the vorticity. After calculating the primary-flow

streamlines, the change in vorticity, or secondary vorticity, can be found. Once the vorticity is known the associated velocity field can be calculated. Had the primary velocity field been the exact solution for the velocity, the calculation of the velocity from the vorticity would have merely given the primary velocity. However, in the case where the primary velocity field is only an approximate guess, the velocity field of the secondary vorticity will result in further deformation of the vortex lines and hence there will be a tertiary vorticity field, which in principle could be calculated, together with its associated velocity field. However, in the case of small upstream vorticity we expect the tertiary (and higher-order) vorticity fields to be negligible.

In recent years increasing attention has been paid to secondary flows in the cardiovascular system and in the lung airways (Lighthill 1972). Of particular importance are the secondary flows which are observed in bifurcating tubes (Schroter & Sudlow 1969). They have the effect of keeping shear rates high on the flow divider and low on the outside walls. The high dissipation rate associated with the high wall shear on the divider implies a greater pressure drop than in Poiseuille flow at the same Reynolds number, the actual value of the pressure drop depending on the strength of the secondary motions (Pedley, Schroter & Sudlow 1973). Furthermore, in blood vessels regions of low wall shear rate may be particularly important in the development of atheroma (Caro, Fitz-Gerald & Schroter 1971). Mixing of gases and solutes in the lungs and blood vessels will also be affected by the strength of secondary motions.

In the first few branches of the lungs and in the aorta, the Reynolds numbers of interest are large, and so in principle we should be able to use an inviscid analysis followed by a boundary-layer analysis. Previous studies of viscous flows in curved tubes are applicable at lower Reynolds numbers (McConalogue & Srivastava 1968). In this paper we present the solution for inviscid flow in a tube of slowly varying ellipticity. The relevance of this type of flow to motion through a bifurcation is explained below. Scherer (1972) has studied inviscid flow through a bifurcation by considering only the development of flow in the daughter tubes and neglecting the details of flow in the bifurcation itself.

The lungs are joined to the larynx by a large tube, the trachea. This bifurcates into two bronchi, which join it to the lobes of the lungs. The bronchi again bifurcate, in an asymmetric manner, for some twenty generations until the smallest tubes, the alveolar ducts, give rise to the alveoli, where gas exchange takes place. The Reynolds number during fairly heavy breathing varies from around 10^4 in the trachea to 10^{-2} in the alveoli. In the arterial network there is a similarly vast range of Reynolds numbers, between the aorta and the finest capillaries. This analysis is therefore expected to apply only to the larger airways and blood vessels, although in the largest of all the assumption of laminar flow is questionable.

In mammals, the flows encountered are usually pulsatile. Suppose that ϖ is a typical frequency of the pulsations of the heart or lung. Let $\bar{U}$ be a velocity scale and l_0 an axial length scale of the region we are interested in. Then quasi-steady flow will exist if

$$\varpi l_0/\bar{U} \ll 1. \tag{1}$$

In the larger airways the flow can be considered quasi-steady. This is also true in the smaller arteries, but in the largest artery, the aorta, because the heart rate is higher than the breathing rate, the flow cannot be considered quasi-steady. The analysis presented here will be a steady-flow analysis and hence will be relevant only to those flows in the lungs and cardiovascular system which can be considered quasi-steady.

Two different types of secondary flow are encountered. In bent tubes the secondary flow which occurs is associated with the turning of the direction of motion of the stream. In channels of constant cross-section, fluid flowing around a bend has generated in itself axial vorticity which is approximately twice the bend angle times the upstream vorticity normal to the plane of the bend (Squire & Winter 1951). However secondary flows also arise in situations where the mean direction of flow does not change but the tube changes in cross-section in a non-axisymmetric manner. In situations where both types of secondary flow occur it is not clear how the two types interact. In the bifurcating tubes encountered in the lungs and cardiovascular system, for example, the parent tube changes in cross-section before it bifurcates. Stehbens (1974) gives details of this change in cross-sectional area for the iliac bifurcation in rabbits, and concludes that study of flow in such regions is necessary for the understanding of the subsequent flow development, and in particular for predicting separation at bifurcations. This study agrees with that conclusion.

Mathematically the problem of flow through a bifurcation appears to be intractable at present. However, a first step in studying such flows is to consider flow through an idealized symmetric bifurcation. Consider a semi-infinite smooth circular cylinder whose cross-sectional shape changes, becoming elliptical. The elliptical cross-section then becomes dumbell shaped and finally two daughter tubes emerge. The branch angle is defined as half the angle between the two daughter tubes. Such a bifurcation is shown in figure 1. Probably the simplest way to tackle flow through such a bifurcation is to divide the flow into the following regions.

(*a*) Region 1–2: a cylinder of slowly varying ellipticity.

(*b*) Region 2–3: occurrence of flow division.

(*c*) Region 3–4: entry flow into daughter tubes.

It is not known how important each of these regions is in the development of secondary flows. The model of Scherer (1972) was applied to flow in the daughter tubes on the assumption that the vorticity at the entrance was known and did not subsequently vary with distance. Thus the axial velocity profile far downstream could be calculated. However, he neglected the secondary motion which could have developed in the region 1–2 and thus a region of great interest is region 3–4, where the axial vorticity is strongly dependent on axial distance. In studying region 1–2 we consider a tube of slowly varying ellipticity as the potential velocity can be easily calculated for such a geometry, and the velocity field simply obtained from the vorticity field.

Potential flow has been considered by Olsen (1971), who derived the first two terms of an expansion for the potential in terms of a parameter representing the slowly varying nature of the tube. Olsen also calculated the Stokes flow in

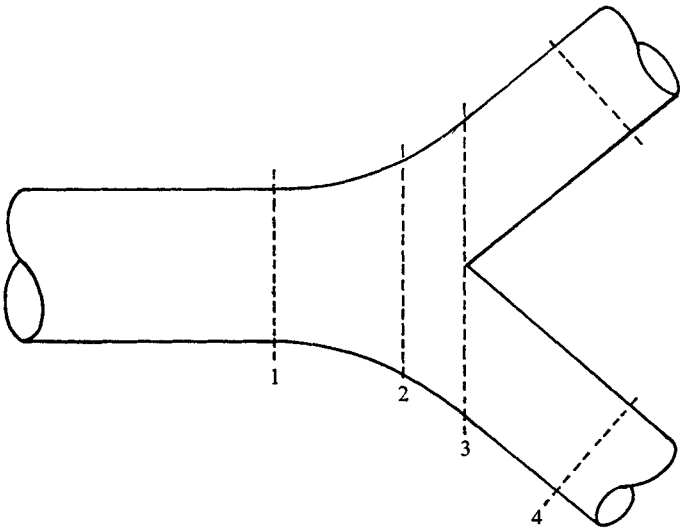

FIGURE 1 Idealized symmetric bifurcation, showing points of onset of changes in geometry. (1) Circular cylinder becomes elliptical. (2) Elliptical cylinder becomes dumbell shaped. (3) Daughter tubes emerge. (4) Daughter tubes become straight circular cylinders.

such a tube and made experimental measurements of such flows. The experiments were performed at several Reynolds numbers, varying from 330 to 2164 (based on the diameter of and average velocity in the parent tube), and for flat and parabolic entrance velocities. As would be expected at these Reynolds numbers, the observations did not agree with the Stokes-flow calculations. Furthermore, the potential-flow analysis was unable to bring out the essential secondary-flow features which were evident in the experimental data. That potential-flow analysis is, however, used in the present paper (see §2) to provide a first approximation on the basis of which the subsequent study of the secondary-flow effects can proceed. In §4 a comparison is made between the experimental observations of Olsen and our secondary-flow calculations. In addition the nature of the flow is calculated for other cases involving changes in the area of the tube.

2. Preliminaries

Here we describe the problem more fully, introduce a non-dimensionalization and present the solution for potential flow (Olsen 1971).

Let $(\hat{x}, \hat{y}, \hat{z})$ be rectangular Cartesian co-ordinates with $\hat{x}$ in the axial direction, and let the boundary of the tube be

$$\hat{y}^2/\hat{a}^2 + \hat{z}^2/\hat{b}^2 = 1, \tag{2}$$

where $\hat{a} = \hat{a}(\hat{x})$, $\hat{b} = \hat{b}(\hat{x})$ and $\hat{a} \to a_0$ and $\hat{b} \to a_0$ as $\hat{x} \to -\infty$. Thus $\hat{a}$ and $\hat{b}$ are respectively the semimajor and semiminor axes of the elliptic cross-section at station x. Assume that the functions a and b vary slowly with $\hat{x}$. Let $\hat{\ell}$ be the

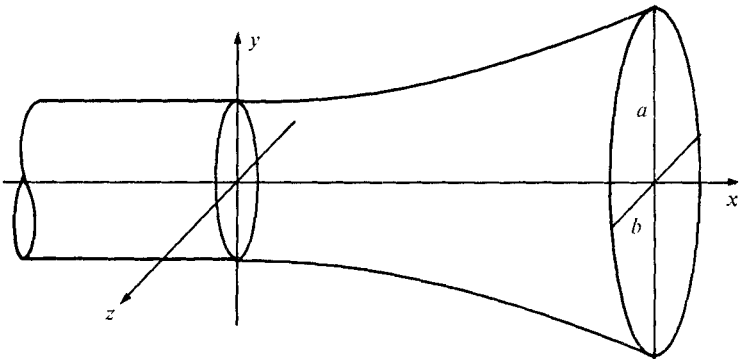

FIGURE 2. Geometry of slowly varying elliptic cylinder.

time and $\hat{\mathbf{u}} = (\hat{u}, \hat{v}, \hat{w})$ be the velocity. Take l_0 to be an axial length scale, $\overline{U}$ to be a velocity scale and choose a time scale $l_0/\overline{U}$.

Define

$$\epsilon = a_0/l_0 \ll 1, \tag{3}$$

and non-dimensionalize according to the following scheme:

$$\left.\begin{aligned} x = \hat{x}/l_0, \quad y = \hat{y}/a_0, \quad z = \hat{z}/a_0, \\ \mathbf{u} = \overline{U}^{-1}\hat{\mathbf{u}}, \\ a = \hat{a}/a_0, \quad b = \hat{b}/a_0, \quad t = \hat{t}\overline{U}/l_0. \end{aligned}\right\} \tag{4}$$

The vorticity scale is $\overline{U}/a_0$. The boundary of the tube is then

$$y^2/a^2 + z^2/b^2 = 1. \tag{5}$$

Let $S = ab$ be the non-dimensional cross-sectional area; far upstream the dimensional area is πa_0^2, downstream it is $\pi a_0^2 S$. The tube geometry is shown in figure 2.

Equations (3) and (4) suggest that the equation for the non-dimensional Laplacian operator should be

$$\nabla^2 = \epsilon^2 \frac{\partial^2}{\partial x^2} + \frac{\partial^2}{\partial y^2} + \frac{\partial^2}{\partial z^2}, \tag{6}$$

with an approximate form

$$\nabla_1^2 = \partial^2/\partial y^2 + \partial^2/\partial z^2, \tag{7}$$

namely the two-dimensional Laplacian in the cross-plane. Let ϕ be the perturbation potential, so that the velocity is

$$\mathbf{u} = S^{-1}\mathbf{i} + \nabla\phi, \tag{8}$$

where $\mathbf{i}$ is a unit vector in the x direction and

$$\nabla = \left(\epsilon \frac{\partial}{\partial x}, \frac{\partial}{\partial y}, \frac{\partial}{\partial z}\right). \tag{9}$$

The continuity equation is

$$\nabla^2\phi = -\epsilon \partial S^{-1}/\partial x \tag{10}$$

and on the boundary of the tube

$$\mathbf{n}.\mathbf{u} = 0, \tag{11}$$

where $\mathbf{n}$ is a unit vector normal to the boundary. The boundary condition far upstream is $\phi \to 0$ as $x \to -\infty$. The potential is found by supposing that ϕ can be represented as

$$\phi = \epsilon\phi_1 + \epsilon^3\phi_2 + O(\epsilon^5). \tag{12}$$

This perturbation procedure produces a series of Neumann problems in the cross-planes x = constant and thus an arbitrary function of x appears at each step. This function must be chosen such that the axial velocity satisfies the flux condition, namely that the volume of fluid passing each station x = constant per unit time is a constant. Olsen (1971) presented the solution for ϕ_1 but did not calculate the arbitrary function of x. The solution is

$$\phi_1 = \frac{1}{2S}\left(\frac{y^2a'}{a} + \frac{z^2b'}{b}\right) - \frac{1}{8}\int_{-\infty}^{x}\left\{a^2\left(\frac{a'}{a^2b}\right)' - b^2\left(\frac{b'}{ab^2}\right)'\right\}dx, \tag{13}$$

where a prime indicates d/dx.

The problem we should like to solve, namely the development of an arbitrary flow which encounters a region in which the boundary shape changes slowly with axial distance, is unfortunately beyond our grasp. It is necessary to assume that far upstream the axial flow is only slightly sheared. Thus we shall take $u \to 1 - \delta r^2$ as $x \to -\infty$, where $\delta \ll 1$ and $r^2 = x^2 + y^2$. Classical secondary-flow methods have been developed which deal with large shear in the oncoming stream but they rely on the deformation of the streamlines being small. If a large deformation occurs, as in the present case, the problem is tractable only if the upstream transverse vorticity is small. This is discussed by Hawthorne (1965).

3. Small vorticity/large deformation solutions

When the flow upstream has only small transverse vorticity one can obtain a solution for flow in a tube of slowly varying ellipticity by using classical secondary-flow methods. Such methods were introduced by Squire & Winter (1951) to analyse the flow of a slightly sheared fluid through a cascade of turbine blades.

Knowing the potential solution, one considers the deformation of vortex lines which are carried by the streamlines of the potential flow. This deformation of the vortex lines produces a secondary flow owing to the generation of streamwise vorticity. Changes in the original axial velocity profile are produced convectively. Such a method of analysis will be valid for small shear upstream and only for a relatively short axial distance. This is because the effect of the secondary flow is to produce further distortion of the vortex lines, generating tertiary vorticity, which in turn produces tertiary flow. The cumulative effect of such action is to cause the secondary-flow theory to become inaccurate far downstream.

One can estimate the 'entrance length' of approximate validity of the secondary-flow theory. Suppose that in travelling an axial distance $O(l)$ a fluid particle is displaced transversely a distance $O(\epsilon l)$ by the primary flow. If the upstream vorticity is $O(\delta)$ then one expects an additional displacement $O(\epsilon\delta l)$ in the

transverse direction from the secondary velocities. When the extra displacement is comparable with the radial dimensions one no longer expects the secondary-flow theory to be reliable. Using $\epsilon = a_0/l_0$ we see that the condition given is

$$l/a_0 = O((\epsilon\delta)^{-1}), \tag{14}$$

which agrees with physical intuition, for as ϵ or δ becomes smaller, the entrance length in which the theory is valid becomes larger.

Let the primary flow be the potential flow given in § 2. The streamlines of the primary flow are calculated from

$$\frac{dy}{dx} = \frac{\phi_y}{\epsilon(S^{-1}+\epsilon\phi_x)}, \quad \frac{dz}{dx} = \frac{\phi_z}{\epsilon(S^{-1}+\epsilon\phi_x)}. \tag{15}$$

Substituting $\phi = \epsilon\phi_1 + O(\epsilon^3)$ with ϕ_1 given by (13), the solution is

$$y = ay_0 + O(\epsilon^2), \quad z = bz_0 + O(\epsilon^2), \tag{16}$$

where (y_0, z_0) is the origin of the streamline as $x \to -\infty$. It can be seen that (16) represents the deformation of transverse circles of fluid particles into ellipses as the fluid flows from a circular tube into an elliptical one.

The t-function, representing the time taken for a fluid particle to reach station x relative to the time it would have taken in an undeformed tube, takes the form

$$t(x, y_0, z_0) = \frac{1}{\epsilon}\left\{x + \int_{-\infty}^{x}\left(\frac{1}{u} - 1\right)dx\right\}. \tag{17}$$

The t-function was first defined by Lighthill (1956) and is given in (17) in the non-dimensional form appropriate to this paper. The secondary vorticity is calculated from the stretching of the vortex lines and was given by Lighthill (1956). If $(\omega_x, \omega_y, \omega_z)$ are the vorticities in the (x, y, z) directions respectively, in non-dimensional form we have

$$\left.\begin{aligned} \omega_x &= \partial w/\partial y - \partial v/\partial z, \\ \omega_y &= \partial u/\partial z - \epsilon\,\partial w/\partial x, \\ \omega_z &= \epsilon\,\partial v/\partial x - \partial u/\partial y. \end{aligned}\right\} \tag{18}$$

Lighthill's equations for the vorticity are

$$\left.\begin{aligned} \omega_x &= u\,\partial(U_0, t)/\partial(y_0, z_0), \\ \omega_y &= v\frac{\partial(U_0, t)}{\partial(y_0, z_0)} - \frac{\partial(U_0, y)}{\partial(y_0, z_0)}, \\ \omega_z &= w\frac{\partial(U_0, t)}{\partial(y_0, z_0)} - \frac{\partial(U_0, z)}{\partial(y_0, z_0)}, \end{aligned}\right\} \tag{19}$$

where $U_0 = U_0(y_0, z_0)$ is the oncoming shear flow. Here we have

$$U_0 = 1 - \delta(y_0^2 + z_0^2). \tag{20}$$

Using the potential axial velocity defined by (8) in (15) we calculate the t-function in the form

$$t = \epsilon^{-1}\{t_0(x) + \epsilon^2 t_1(x, y_0, z_0) + O(\epsilon^4)\}. \tag{21}$$

We express the velocities as perturbation expansions in ϵ and δ according to the following scheme:

$$\left.\begin{aligned} u &= S^{-1} + \delta u_1 + \epsilon^2 \phi_{1x} + \delta^2 u_2 + O(\epsilon^4), \\ v &= \epsilon \phi_{1y} + \epsilon\delta v_1 + O(\epsilon^3), \\ w &= \epsilon \phi_{1z} + \epsilon\delta w_1 + O(\epsilon^3), \end{aligned}\right\} \tag{22}$$

where ϕ_1 is the perturbation potential given by (13). There is no $O(\epsilon\delta)$ term in the expansion for u since no term of this order appears in the expressions for the secondary vorticity given below, as t_0 is a function of x alone.

Let the actual streamlines, rather than the primary streamlines, be

$$\left.\begin{aligned} y &= ay_0 + \delta\eta(x, y_0, z_0) + O(\epsilon^2), \\ z &= bz_0 + \delta\zeta(x, y_0, z_0) + O(\epsilon^2). \end{aligned}\right\} \tag{23}$$

Substituting (21)–(23) into the expressions (19) for the secondary vorticity we obtain

$$\left.\begin{aligned} \omega_x &= -2\epsilon\delta \frac{1}{S}\left(y_0 \frac{\partial t_1}{\partial z_0} - z_0 \frac{\partial t_1}{\partial y_0}\right) + O(\delta^2), \\ \omega_y &= -2\delta a z_0 + 2\delta^2 \left(y_0 \frac{\partial \eta}{\partial z_0} - z_0 \frac{\partial \eta}{\partial y_0}\right) + O(\epsilon^2\delta), \\ \omega_z &= 2\delta b y_0 + 2\delta^2 \left(y_0 \frac{\partial \zeta}{\partial z_0} - z_0 \frac{\partial \zeta}{\partial y_0}\right) + O(\epsilon^2\delta^2). \end{aligned}\right\} \tag{24}$$

In order that the tertiary vorticity be small compared with the secondary vorticity, we see that the ω_x equation in (24) requires

$$\delta = o(\epsilon). \tag{25}$$

At this point η and ζ are still unknown and represent the effect on the primary streamlines of the developing secondary flow. The method of solution is to ignore the $O(\delta^2)$ terms in ω_x when calculating the lowest-order perturbation (u_1, v_1, w_1). Then using v_1 and w_1 in (15) allows η and ζ to be calculated, and hence u_2. The second-order axial-velocity term u_2 will give the redistribution of axial momentum due to the secondary motions.

To calculate the velocities from the vorticity we use

$$\nabla^2 \mathbf{u} = -\nabla \times \boldsymbol{\omega}, \tag{26}$$

where $\boldsymbol{\omega}$ is the vorticity vector. The t-function by (8), (13) and (17) is

$$t(x, y_0, z_0) = \frac{1}{\epsilon}\left\{x + \int_{-\infty}^{x} (S-1)\,dx\right\} - \frac{\epsilon}{2}\left\{y_0^2 \int_{-\infty}^{x} a^2 S^2 Y'\,dx + z_0^2 \int_{-\infty}^{x} b^2 S^2 Z'\,dx - G(x)\right\}, \tag{27}$$

where

$$Y = a'/aS, \quad Z = b'/bS,$$

$$G(x) = \frac{1}{4}\int_{-\infty}^{x} (a^2 Y' + b^2 Z')\, S^2\,dx.$$

Define

$$c(x) = \int_{-\infty}^{x} S^2 (a^2 Y' - b^2 Z')\,dx.$$

Then the components of the vorticity (24) become

$$\left.\begin{aligned}\omega_x &= -2\epsilon\,\delta c(x)/S^2+O(\delta^2),\\ \omega_y &= -2\delta a^2 z/S+O(\delta^2),\\ \omega_z &= 2\delta b^2 y/S+O(\delta^2).\end{aligned}\right\} \tag{28}$$

Taking the curl of the vorticity we see that the equations for the coefficients u_1, v_1 and w_1 in (22) are

$$\left.\begin{aligned}\nabla_1^2 u_1 &= -2S(a^{-2}+b^{-2}),\\ \nabla_1^2 v_1 &= -2(Y-Z)\,b^2 y+2cy/S^2,\\ \nabla_1^2 w_1 &= 2(Y-Z)\,a^2 z-2cz/S^2.\end{aligned}\right\} \tag{29}$$

The last terms in the equations for v_1 and w_1 in (29) represent trailing vorticity in the sense that should the wall slope become zero, so that the circular cylinder has become an elliptic cylinder, there would be axial vorticity downstream given by these terms. The other terms in (29) are transient since they contribute to the secondary vorticity only whilst the tube is actually changing in cross-section. The boundary conditions are that upstream the secondary motions vanish and a consistent expansion in ϵ and δ of the inviscid boundary condition that there be no velocity normal to the wall. Hence, if the surface is

$$\begin{gathered}f(x,y,z)\equiv 0,\\ f_x u_1+f_y v_1+f_z w_1=0 \quad \text{on} \quad f\equiv 0.\end{gathered} \tag{30}$$

The continuity equation is represented by the flux condition mentioned earlier.

The velocity field given by (29) is found in two parts. First the velocity field $(0, v_2, w_2)$ due to the 'trailing vorticity' is found using a stream function which vanishes on the boundary, hence automatically satisfying the condition that there be no velocity component normal to the wall. The second part, the velocity (u_1, v_2, w_3) due to transient terms, requires the introduction of further potential solutions.

The solution of $\quad \nabla_1^2 v_2 = 2cy/S^2, \quad \nabla_1^2 w_2 = -2cz/S^2 \quad (31)$

which satisfies the boundary conditions is

$$v_2=\psi_z, \quad w_2=-\psi_y, \tag{32}$$

where

$$\psi=\frac{1}{3}\frac{c}{a^2+b^2}yz\left(\frac{y^2}{a^2}+\frac{z^2}{b^2}-1\right). \tag{33}$$

The solution of

$$\left.\begin{aligned}\nabla_1^2 u_1 &= -2S(a^{-2}+b^{-2}),\\ \nabla_1^2 v_3 &= -2(Y-Z)\,b^2 y,\\ \nabla_1^2 w_3 &= 2(Y-Z)\,a^2 z\end{aligned}\right\} \tag{34}$$

which satisfies the boundary conditions is

$$\left.\begin{aligned}u_1 &= \{F-S(y^2/a^2+z^2/b^2)\},\\ v_3 &= -\tfrac{1}{3}y\{(Y-Z)\,b^2y^2+2YS^2+ZS^2-3SYF\},\\ w_3 &= \tfrac{1}{3}z\{(Y-Z)\,a^2z^2+YS^2+2ZS^2-3SZF\},\end{aligned}\right\} \tag{35}$$

where

$$F=(S^2-1)/2S.$$

Thus we have evaluated all the terms in (22) except $\delta^2 u_2$, which is due to convection of transverse vorticity by the secondary-flow streamlines. Thus it is necessary to return to (15) and evaluate the $O(\delta)$ term represented in (23) by η and ζ. The $O(\delta)$ change in the streamlines will lead to an $O(\delta^2)$ term in the transverse vorticity and hence an $O(\epsilon\delta^2)$ term in the transverse velocities. We intend to calculate only the $O(\delta^2)$ term in the axial velocity.

If the secondary velocities are known the perturbation to the primary streamlines can be calculated. We have, using (22) in (15),

$$\left.\begin{aligned} dy/dx &= S\phi_{1y} + \delta S(v_1 - S\phi_{1y}u_1) + O(\epsilon^2), \\ dz/dx &= S\phi_{1z} + \delta S(w_1 - S\phi_{1z}u_1) + O(\epsilon^2). \end{aligned}\right\} \tag{36}$$

The transverse velocities v_1 and w_1 calculated above are simply $v_1 = v_2 + v_3$ and $w_1 = w_2 + w_3$. Solving (36) we evaluate η and ζ as

$$\left.\begin{aligned} \eta &= \tfrac{1}{3}ay_0\{\alpha_1(x)\,(y_0^2 - 1) + \alpha_2(x)\,z_0^2\}, \\ \zeta &= \tfrac{1}{3}bz_0\{\beta_1(x)\,y_0^2 + \beta_2(x)\,(z_0^2 - 1)\}, \end{aligned}\right\} \tag{37}$$

where

$$\alpha_1(x) = \int_{-\infty}^{x} \left(2YS^3 + ZS^3 + \frac{cS}{a^2+b^2}\right) dx, \tag{38a}$$

$$\alpha_2(x) = 3\int_{-\infty}^{x} \left(YS^3 + \frac{cS}{a^2+b^2}\right) dx, \tag{38b}$$

$$\beta_1(x) = 3\int_{-\infty}^{x} \left(ZS^3 + \frac{cS}{a^2+b^2}\right) dx, \tag{38c}$$

$$\beta_2(x) = \int_{-\infty}^{x} \left(YS^3 + 2ZS^3 - \frac{cS}{a^2+b^2}\right) dx. \tag{38d}$$

Thus the transverse secondary vorticity is

$$\left.\begin{aligned} \omega_y &= -2\delta a^2 z/S - \frac{2\delta^2 a}{3}\left\{(\alpha_2 - \beta_2)\left(\frac{z}{b}\right)^3 + (\beta_2 - \alpha_1)\left(\frac{z}{b}\right)\right\}, \\ \omega_z &= 2\delta b^2 y/S + \frac{2\delta^2 b}{3}\left\{(\beta_1 - \alpha_1)\left(\frac{y}{a}\right)^3 + (\alpha_1 - \beta_2)\left(\frac{y}{a}\right)\right\}. \end{aligned}\right\} \tag{39}$$

Define

$$\gamma(x) = 2\int_{-\infty}^{x} \left(YS^3 - ZS^3 + \frac{cS}{a^2+b^2}\right) dx, \tag{40}$$

$$\tau(x) = \int_{-\infty}^{x} \left(YS^3 - ZS^3 + \frac{2cS}{a^2+b^2}\right) dx. \tag{41}$$

Consider which velocity terms can give rise to $O(\delta^2)$ transverse vorticity. Clearly any transverse-vorticity terms would be $O(\delta^2/\epsilon)$, however since these are absent we deduce that the $O(\delta^2)$ transverse vorticity is associated entirely with an $O(\delta^2)$ axial-velocity term. Hence we calculate

$$u_2 = \tfrac{1}{3}S\tau\left(\frac{z^2}{b^2} - \frac{y^2}{a^2}\right) - \tfrac{1}{6}S\gamma\left(\frac{z^4}{b^4} - \frac{y^4}{a^4}\right). \tag{42}$$

The addition of u_2 to the axial velocity does not affect the flux of fluid passing any station and hence there is no non-zero function of x to be added to u_2.

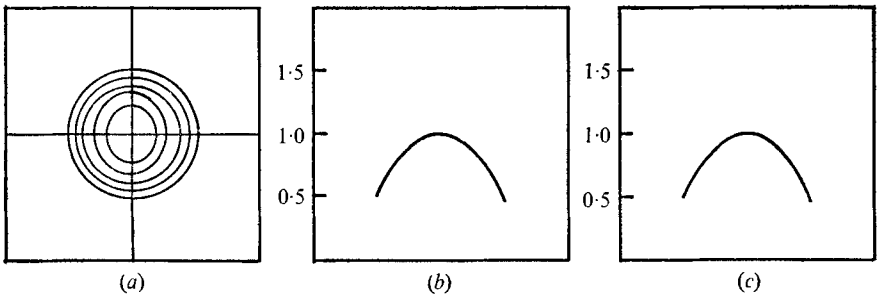

FIGURE 3. Initial axial velocity profile. (*a*) Contours of constant axial velocity at 0·5(0·1)1. (*b*) Velocity profile on semimajor axis (*c*) Velocity profile on semiminor axis.

4. Examples: comparison with experiment

Olsen (1971) observed flow through a tube of varying ellipticity at Reynolds numbers based on tube diameter and average velocity between 330 and 2164. The tube was constructed such that the radius of curvature of $y = a(x)$ was 5; thus for $x > 0$, $y = a(x)$ was the arc of a circle centre (0, 6) and radius 5 units, and $a(x) = 1$ for $x < 0$. The tube was of constant cross-sectional area thus $b(x) = 1/a(x)$. Calculations of the velocity field have been made for this geometry and are shown in figures 3–6. These calculations were made for $\epsilon = 0{\cdot}5$ and $\delta = 0{\cdot}5$. The value of ϵ is that used by Olsen and δ was chosen as 0·5 so that (i) secondary flows would develop reasonably quickly with axial distance, (ii) near the centre of the tube the inlet velocity profile would model Poiseuille-flow inlet conditions and (iii) the terms neglected in the ϵ, δ expansion of the velocity field would still be approximately an order of magnitude smaller than those calculated. In figure 3 the initial axial velocity profile is shown, contours of axial velocity being drawn at $u = 0{\cdot}5(0{\cdot}1)1$. Figure 4 shows the secondary velocities at $x = 1$ together with the axial velocities on the semimajor and semiminor axes and the contours of axial velocity. Figure 5 shows the same quantities for $x = 2$ and figure 6 shows the axial velocity at $x = 2{\cdot}5$. It can be seen that the development of the axial velocity profile proceeds as follows. The circular rings of fluid travelling with the same axial velocity are initially deformed into ellipses as the fluid first enters the elliptic region, however, further downstream, the secondary velocities cause fluid to move in the opposite direction to the primary transverse flow, distorting the elliptical rings of fluid into the shapes shown in figures 5 and 6. The primary and secondary streamlines are shown schematically in figure 7, together with the decomposition of the transverse velocities into a primary and a secondary field.

These calculations are compared with the observations of Olsen in figures 8 and 9. In figure 8 the secondary velocities measured by Olsen are compared with the calculated ones for unit flux through the tube, in which the primary axial velocity far upstream is $u = \frac{4}{3}(1 - \delta r^2)$. It can be seen that, ignoring the boundary layer, the explanation of the composition of the transverse velocities is qualitatively correct. Further, the theory gives quantitatively correct magnitudes for the transverse velocities.

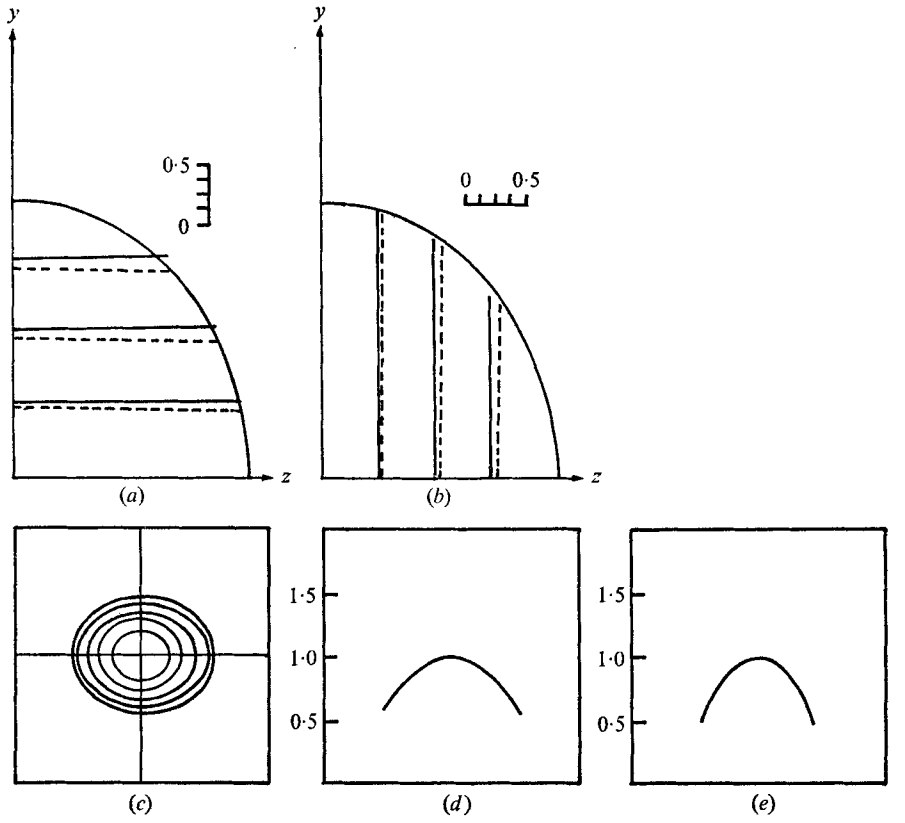

FIGURE 4. Velocity field at $x = 1$. (*a*) Transverse motions in direction of semimajor axis. (*b*) Transverse motions in direction of semiminor axis. (*c*) Contours of constant axial velocity at 0·5(0·1)1. (*d*) Velocity profile on semimajor axis. (*e*) Velocity profile on semiminor axis. Non-dimensional velocity scales shown.

The transverse velocities for flat inlet flow are larger than those for parabolic flow. This has two causes: first, the local velocity near the wall is larger for the case of a flat inlet velocity and hence the potential contribution to the transverse velocities is large, and second, the boundary layer which develops is a region of large vorticity and hence locally the deformation of the vortex lines leads to large axial vorticity.

In figure 9 the axial velocity profiles measured by Olsen at $x = 1{\cdot}625$ and $x = 2{\cdot}375$ are compared with the theoretical curves. In the core, away from the boundary layer at the wall, the curves are qualitatively correct. In particular the velocity profile in the direction of the semiminor axis becomes 'plug' shaped whilst the profile in the direction of the semimajor axis develops an inflexion point. Both of these phenomena are observed experimentally. However, the region in which the inflexion point is calculated to occur is some distance downstream, where the theory may be of doubtful accuracy and where the disturbance boundary layer may be quite thick. Thus a boundary-layer theory is necessary to complete the model of flow in a slowly varying elliptic tube.

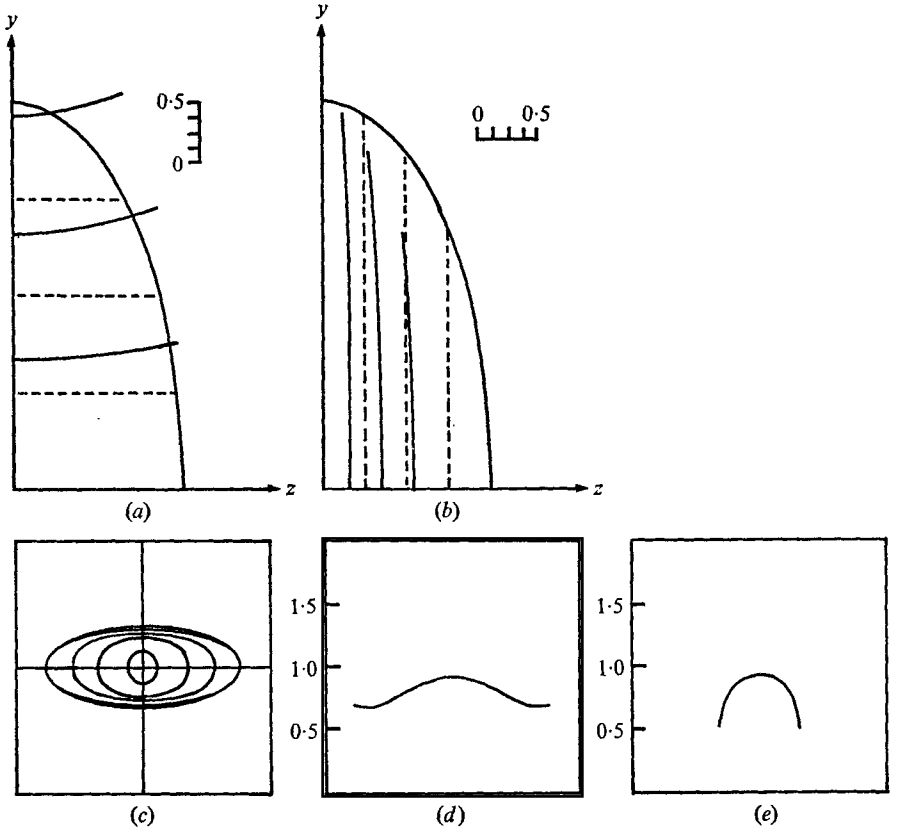

FIGURE 5. Velocity field at $x = 2$. (*a*) Transverse motions in direction of semimajor axis. (*b*) Transverse motions in direction of semiminor axis. (*c*) Contours of constant axial velocity at 0·5(0·1)1. (*d*) Velocity profile on semimajor axis. (*e*) Velocity profile on semiminor axis.

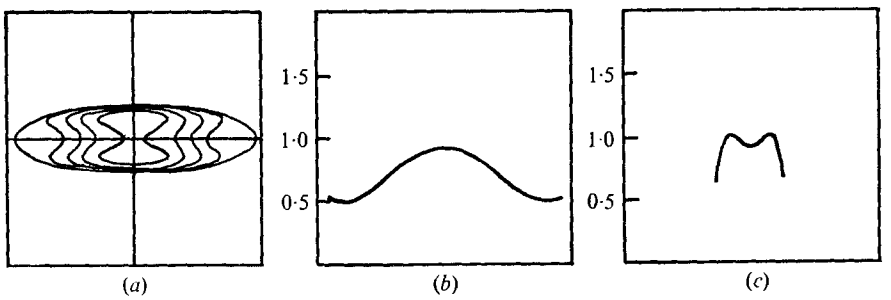

FIGURE 6 Axial velocity field at $x = 2{\cdot}5$. (*a*) Contours of constant axial velocity at 0·5(0·1)1. (*b*) Velocity profile on semimajor axis. (*c*) Velocity profile on semiminor axis.

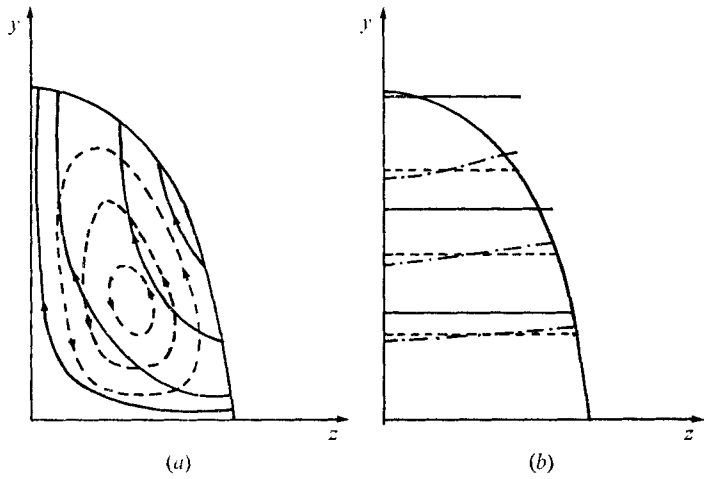

FIGURE 7. Schematic structure of secondary motions in a slowly varying elliptic cylinder. (*a*) Streamlines due to transverse motion projected onto one plane: ———, potential-flow streamlines; – – – – –, secondary-vorticity streamlines. (*b*) Structure of secondary velocities in direction of semimajor axis: ———, potential velocity; —·—·—, secondary-vorticity velocity.

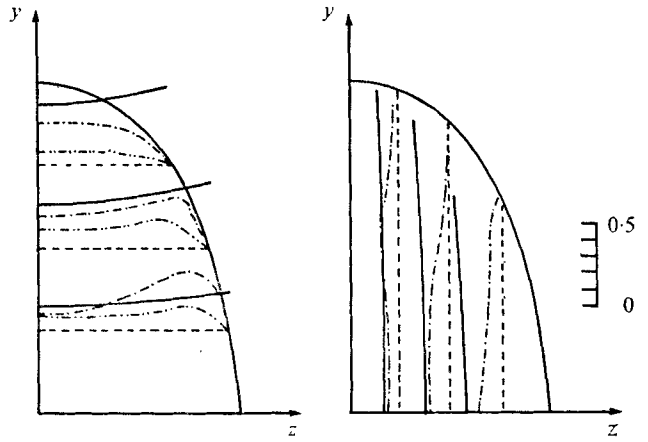

FIGURE 8. Comparison of theoretical transverse velocities calculated for $\epsilon = \frac{1}{2}$, $\delta = \frac{1}{2}$ with velocities measured by Olsen (1971). ———, theoretical; —·—·—, flat inlet axial velocity; —·—·—·—, parabolic inlet axial velocity. Measurements made at $x = 1{\cdot}625$.

Calculations for cases of increasing and decreasing area show that there are two factors which influence the flow development. First, the changing ellipticity induces secondary transverse velocities and these lead to a redistribution of axial momentum giving the profiles which are described above. However, changes in area cause a general stretching (or compression) of vortex lines in the transverse direction and this causes a strengthening (or weakening) of the transverse vorticity without the development of strong secondary motions. Figure 10 shows the development of the axial velocity profile for a case of increasing area whilst

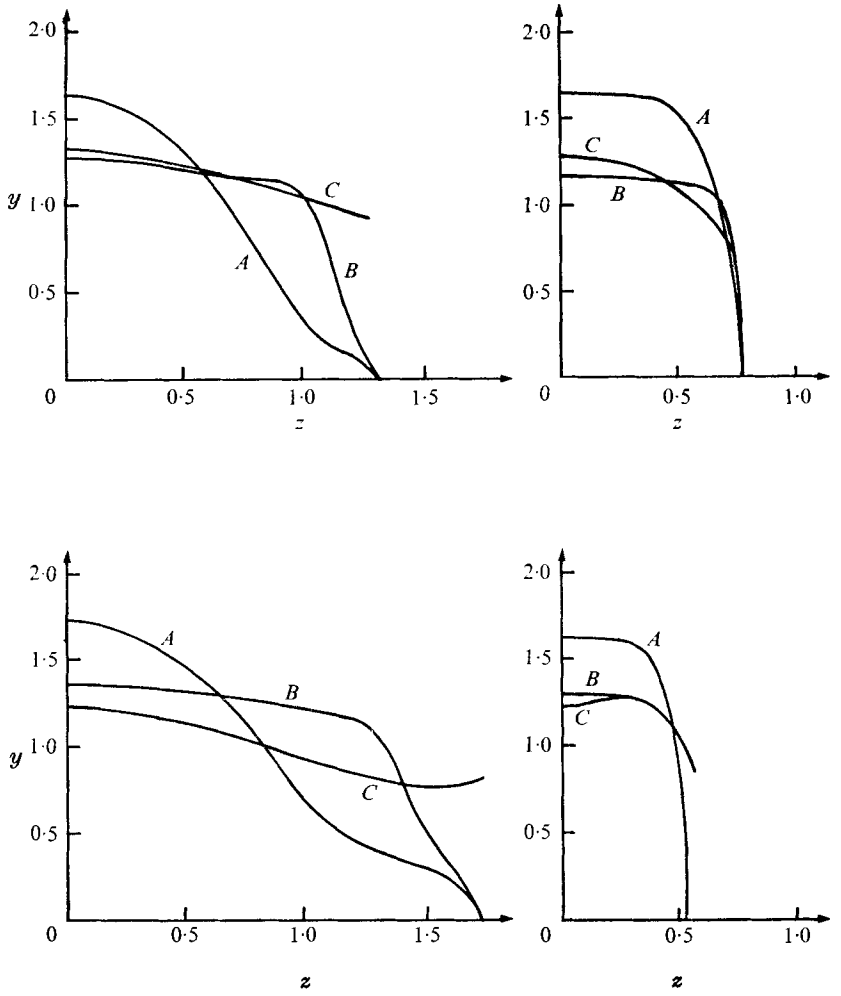

FIGURE 9. Comparison of theoretical axial velocity profiles calculated for $\epsilon = \frac{1}{2}$, $\delta = \frac{1}{2}$ with velocities measured by Olsen (1971). (*a*), (*b*) $x = 1{\cdot}65$. (*c*), (*d*) $x = 2{\cdot}375$. *A*, parabolic axial entrance velocity profile; *B*, flat axial entrance velocity profile; *C*, theoretical axial velocity profiles.

figure 11 shows the effect of decreasing the rate of change of the ellipticity but keeping the rate of area increase the same. It can be seen that the secondary flows must be much more developed in the case of figure 10 than in the case of figure 11. Figure 12 shows the effect of decreasing the area: the transverse vorticity decreases and the axial velocity profiles become plug like.

5. Conclusion

We have used inviscid secondary-flow methods to study the development of flow in a tube which resembles the initial part of a bifurcating tube. Providing the secondary-flow problem can be made tractable, the resulting solutions are

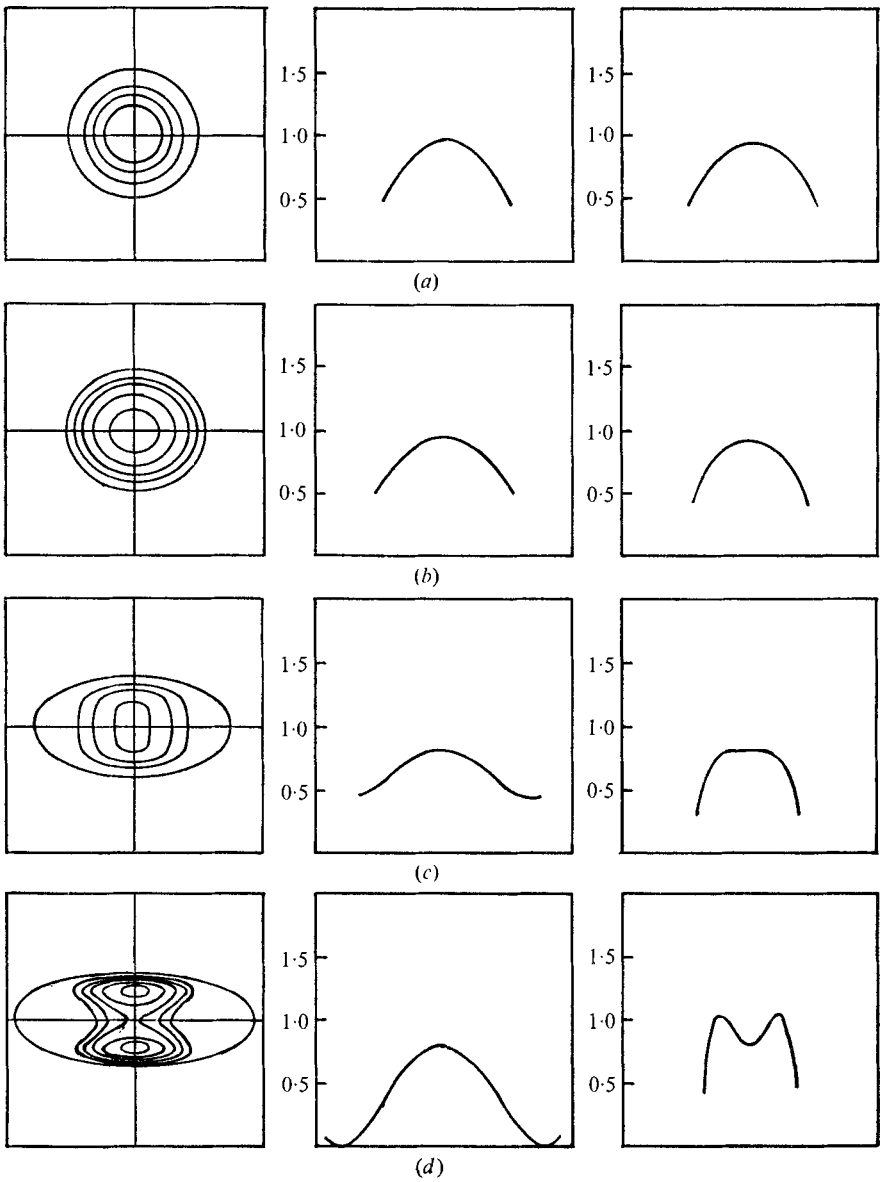

FIGURE 10. Axial velocity field for case of increasing area $b = a^{-\frac{1}{2}}$, where a is taken from Olsen's model. From left to right: contours of constant axial velocity, velocity profile on semimajor axis and velocity profile on semiminor axis. (*a*) $x = 0$. (*b*) $x = 1$. (*c*) $x = 2$. (*d*) $x = 2{\cdot}5$.

sufficiently simple to be used in further work. Such velocity fields could, for instance, be used to study the deposition due to impaction on the tube walls of particles carried by the fluid. Further work to develop a complementary boundary-layer theory is being carried out.

In flow through a slowly varying elliptic tube the deformation of the vortex

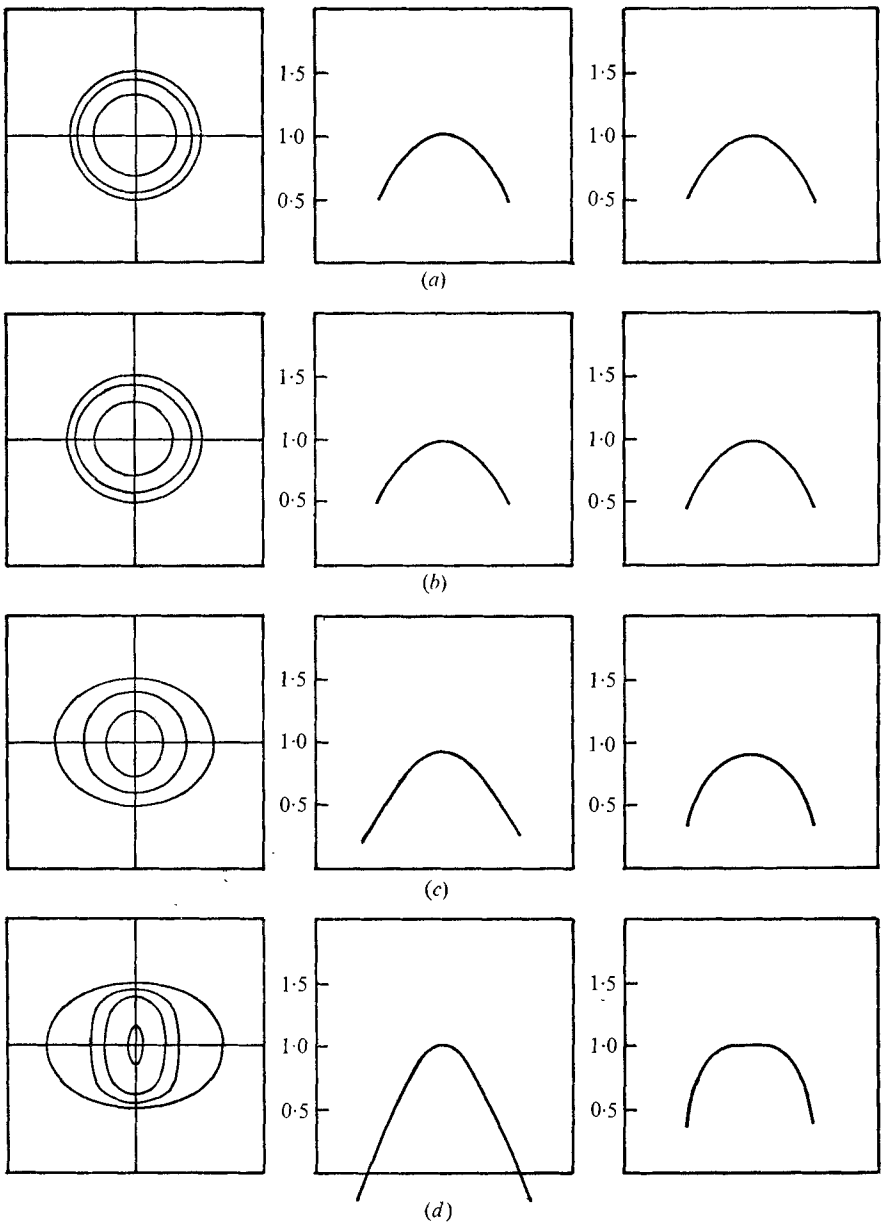

FIGURE 11. Axial velocity field for case of increasing area $b = 1$, area $= a^{\frac{1}{2}}$, where a is taken from Olsen's model. From right to left: contours of constant axial velocity, velocity profile on semimajor axis and velocity profile on semiminor axis. (*a*) $x = 0$. (*b*) $x = 1$. (*c*) $x = 2$. (*d*) $x = 2{\cdot}5$.

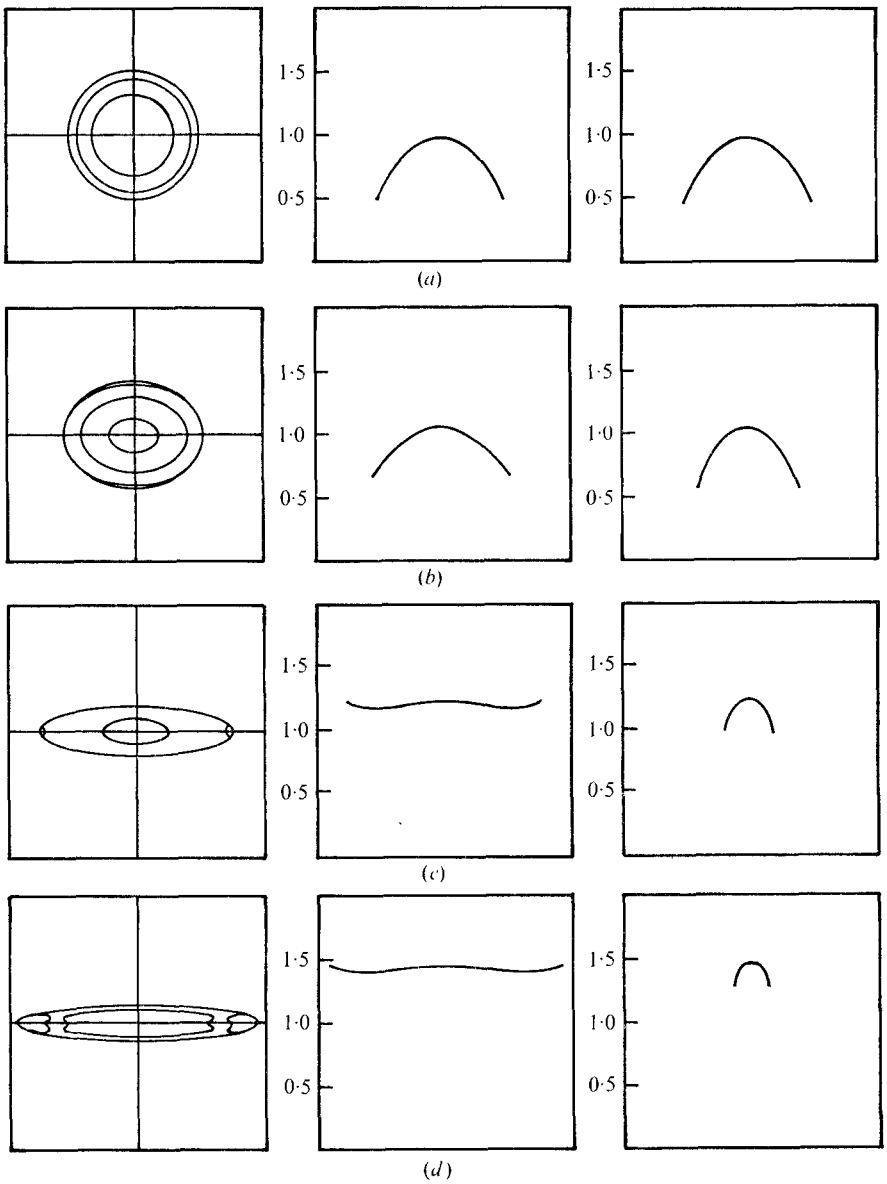

FIGURE 12. Axial velocity field for case of decreasing area $b = a^{-2}$, where a is taken from Olsen's model. From right to left: contours of constant axial velocity, velocity profile on semimajor axis and velocity profile on semiminor axis. (*a*) $x = 0$. (*b*) $x = 1$. (*c*) $x = 2$. (*d*) $x = 2{\cdot}5$.

lines results in transverse velocities which have a characteristic profile, that of circulatory flow in each quadrant of the elliptical cross-section, superposed on the potential flow. Further, the axial velocity profile is distorted, the profile on the semiminor axis becoming plug like, whilst the profile on the semimajor axis develops an inflexion point owing to the transfer of axial momentum by the

transverse motions of the fluid. Comparison with experimental results confirms this picture of the structure of the velocity field.

Thus in considering flow in a bifurcation one has to take the above picture into account. Hence secondary flows in the daughter tubes could be expected to develop more quickly than secondary flows in a curved tube. Further, in the lungs, on expiration, the secondary motions generated as the fluid moves through the daughter tubes into the mother tube would be strengthened in the region of changing tube geometry. Near the ends of the semimajor axis it is apparent that a deceleration of the fluid occurs and a point of inflexion develops in the axial velocity profile. This would lead one to believe that flow could separate in this region, however, further work on developing a boundary-layer theory is necessary before anything further can be said. Also, one would expect that the development of an inflexion point in the axial velocity profile would tend to destabilize the flow. This is in contrast to the situation in a bent pipe, where the flow is more stable than in a straight pipe (Taylor 1929). Experimental evidence confirms the view that flow through a bifurcation is less stable than flow through a straight tube of equivalent calibre (Stehbens 1959; Dekker 1961; West & Hugh-Jones 1959).

I am grateful to Dr T. J. Pedley and Professor Sir James Lighthill for suggesting the problem and invaluable advice during the preparation of the manuscript. I should also like to thank Professor J. H. Horlock and Dr R. C. Schroter for their advice. I acknowledge receipt of a Commonwealth of Australia, CSIRO post-graduate scholarship.

REFERENCES

Caro, C. G., Fitz-Gerald, J. M. & Schroter, R. C. 1971 *Proc. Roy. Soc.* B **177**, 109.
Dekker, E. 1961 *J. Appl. Physiol.* **16**, 1060.
Hawthorne, W. R. 1965 *Research Frontiers in Fluid Dynamics* (ed. Seeger). Interscience.
Horlock, J. H. & Lakshminarayana, B. 1973 *Ann. Rev. Fluid Mech.* **5**, 247.
Lakshminarayana, B. & Horlock, J. H. 1973 *J. Fluid Mech.* **59**, 97.
Lighthill, M. J. 1956 *J. Fluid Mech.* **1**, 31.
Lighthill, M. J. 1972 *J. Fluid Mech.* **52**, 475.
McConalogue, D. J. & Srivastava, R. S. 1968 *Proc. Roy. Soc.* A **307**, 37.
Olsen, D. E. 1971 Ph.D. thesis, Imperial College, London.
Pedley, T. J., Schroter, R. C. & Sudlow, M. F. 1973 *Resp. Physiol.* **9**, 371.
Scherer, P. W. 1972 *J. Biomech.* **5**, 223.
Schroter, R. C. & Sudlow, M. F. 1969 *Resp. Physiol.* **7**, 347.
Squire, H. B. & Winter, K. G. 1951 *J. Aero Sci.* **18**, 271.
Stehbens, W. E. 1959 *Quart. J. Exp. Physiol.* **44**, 110.
Stehbens, W. E. 1974 To be published.
Taylor, G. I. 1929 *Proc. Roy. Soc.* A **124**, 243.
West, J. B. & Hugh-Jones, P. 1959 *J. Appl Physiol* **14**, 753